DALTON

Mercury–osmium carbonyl clusters resulting from facile Hg–C bond cleavage: reactions of $[Os_3H_2(CO)_{10}]$ with $[Hg(C{\equiv}CPh)_2]$ and $[RHgC{\equiv}CHgR]$ (R = Ph, Me or Et)

Yat-Kun Au and Wing-Tak Wong *

Department of Chemistry, The University of Hong Kong, Pokfulam Road, Hong Kong

Reaction of the unsaturated cluster $[Os_3H_2(CO)_{10}]$ with $Hg(C{\equiv}CPh)_2$ afforded two new Os–Hg clusters *cis*-$[Os(CO)_4\{(\mu\text{-}Hg)Os_3(CO)_{10}(\mu\text{-}\eta^2\text{-}CH{=}CHPh)\}_2]$ **1** and $[\{Os_3(CO)_{10}(\mu\text{-}\eta^2\text{-}CH{=}CHPh)\}_2(\mu_4\text{-}Hg)]$ **2** in 30 and 20% yield, respectively. Cluster **1** consists of two $(\mu\text{-}Hg)Os_3(CO)_{10}(\mu\text{-}\eta^2\text{-}CH{=}CHPh)$ subunits bonded to a central $Os(CO)_4$ moiety in the *cis* configuration which under ambient conditions converts into **2** over 3–5 d with the extrusion of a $HgOs(CO)_4$ unit. Cluster **2** comprises two skewed Os–Hg metal butterflies sharing a common wingtip Hg atom. In refluxing tetrahydrofuran (66 °C) **2** underwent redistribution with the symmetrical mercurials $[Hg\{M(CO)_3(\eta^5\text{-}C_5H_5)\}_2]$ (M = Cr, Mo or W) to afford respectively the heterometallic clusters $[\{Os_3(CO)_{10}(\mu\text{-}\eta^2\text{-}CH{=}CHPh)\}(\mu_3\text{-}Hg)\{M(CO)_3(\eta^5\text{-}C_5H_5)\}]$ (M = Cr **3**, Mo **4** or W **5**) in moderate yield. Alternatively, **3**–**5** can be obtained more readily from the reaction of cluster **1** with the corresponding symmetric mercurials at room temperature. Reactions of $[Os_3H_2(CO)_{10}]$ with $[RHgC{\equiv}CHgR]$ (R = Ph, Me or Et) afforded the clusters $[\{Os_3(CO)_{10}(\mu\text{-}\eta^2\text{-}CH{=}CH_2)\}(\mu_4\text{-}Hg)\{Os_3(CO)_{10}(\mu\text{-}H)\}]$ **6** (12%) and $[\{Os_3(CO)_{10}(\mu\text{-}\eta^2\text{-}CH{=}CH_2)\}_2(\mu_4\text{-}Hg)]$ **7** (25%). Cluster **7** is isostructural with **2**, whilst **6** bears a central Hg atom connecting two structurally different osmium triangles. Clusters **1**, **2**, **6** and **7** all result from Hg–C bond cleavage of the parent organomercury species, hence the generality of this cleavage is demonstrated. The new clusters **1**, **2**, **4**, **6** and **7** have been fully characterised by both spectroscopic and crystallographic techniques.

Organomercury fragments which readily attach to a variety of transition metals have been used as building blocks in mixed-metal clusters as well as in the syntheses of high-nuclearity clusters.[1–10] It is anticipated that mixed-metal frameworks containing metal atoms (or cluster subunits) with substantially different electronic properties to those of the principal core can introduce intrinsic metal–metal bond polarity where the potential to induce chemical changes at the interfaces between these subunits would be greatly enhanced. Furthermore, mercury atoms are good 'linkers' in a variety of metal-chain structures,[11–14] as manifested in their ability to participate in a range of multicentre metal–metal bonds. Consequently, the co-ordination as well as the organometallic chemistry of the element are greatly extended.[15–18] The recently reported photochemical reactivity in $[Os_{18}Hg_3C_2(CO)_{42}]^{2-}$ has also revealed that it is possible to open up new synthetic routes to chemical species and novel metal frameworks which are inaccessible by conventional methods.[19–21] In this paper we report our work on the syntheses of a number of new mercury–osmium mixed-metal carbonyl clusters to which little attention has been paid previously. We would like to investigate whether the novel Hg–C bond cleavage, as reported by us recently,[22] is general for other aliphatic and aromatic organomercury species on reacting with triosmium metal clusters. It is hoped that, if the reaction is a general one, new synthetic pathways for certain novel mercury species may be developed which would render them suitable as building blocks for the syntheses of higher-nuclearity mercury mixed-metal clusters.

Recently, a number of asymmetric mercurials comprising the metal core $M_3(\mu_3\text{-}Hg)M'$ such as $[(\mu_3\text{-}C{\equiv}CCMe_3)(OC)_9M_3(\mu_3\text{-}Hg)M']$ [M = Ru or Os; M′ = $Fe(CO)_2(\eta^5\text{-}C_5H_5)$, $Ru(CO)_2(\eta^5\text{-}C_5H_5)$, $Mo(CO)_3(\eta^5\text{-}C_5H_5)$ or $Co(CO)_4$] have been synthesised,[16,23,24] *via* the halide displacement from $[M_3(\mu_3\text{-}Hg)X]$ (X = halide) using certain carbonylmetalate anions Na^+M^- (Scheme 1). It has also been reported that the asymmetric mercurials MHgX (M = mono- or bi-nuclear transition-metal fragment; X = halide or polymetallic fragment) can be prepared by redistribution of the symmetric mercurials HgX_2 and M_2Hg (Scheme 2).[25,26] Both of these results have led us to prepare the asymmetric mercurials $M_3(\mu_3\text{-}Hg)M'$ *via* the redistribution of four-co-ordinated mercury complexes.

$$[M_3(\mu_3\text{-}Hg)X] + Na^+M' \longrightarrow [M_3(\mu_3\text{-}Hg)M'] + Na^+X^-$$

Scheme 1 Formation of asymmetric mercurials of the type $M_3(\mu\text{-}Hg)M'$. X = Cl or Br

$$M_2Hg + HgX_2 \rightleftharpoons 2\,MHgX$$

Scheme 2 Redistribution reaction of symmetric mercurials

Experimental

General conditions

All manipulations were carried out under a dinitrogen atmosphere using standard Schlenk techniques, unless stated otherwise. Solvents were of reagent grade and were distilled from appropriate drying agents and stored under nitrogen prior to use. Products were isolated by preparative thin-layer chromatography (TLC) on silica gel (type 60) GF_{254} Merck 7730 in air.

Instrumentation

Infrared spectra were recorded on a Bio-Rad FTS-7 or a Nicolet 20 SXC FT-IR spectrophotometer in CH_2Cl_2, mass spectra on a Finnigan MAT 95 spectrometer with positive fast atom bombardment (FAB) techniques using *m*-nitrobenzoyl alcohol as matrix, and ^1H NMR spectra on JEOL GSX 270 and Bruker 300 DPX FT-NMR spectrometers in CD_2Cl_2, $CDCl_3$ and $(CD_3)_2CO$ with $SiMe_4$ as internal reference at room temperature.

Reagents

The compounds $Hg(C{\equiv}CPh)_2$,[27] $RHgC{\equiv}CHgR$ (R = Ph, Me

or Et)[28] and $[Hg\{M(CO)_3(\eta^5\text{-}C_5H_5)\}_2]$ (M = Cr, Mo or W)[29] were prepared as in the literature. The cluster $[Os_3H_2(CO)_{10}]$ was synthesised according to a modified procedure.[30] The compounds $[Os_3(CO)_{12}]$, $[M(CO)_6]$ (M = Cr, Mo or W), phenylacetylene, phenylmercury(II) chloride and mercury(II) cyanide were all obtained commercially (Strem) and used as received. Trimethylamine *N*-oxide was sublimed before use.

Reaction of $[Os_3H_2(CO)_{10}]$ with $Hg(C{\equiv}CPh)_2$

A purple solution of $[Os_3H_2(CO)_{10}]$ (50 mg, 0.058 mmol) in CH_2Cl_2 (20 cm^3) was stirred with 1 equivalent of $Hg(C{\equiv}CPh)_2$ (23.35 mg) under N_2. The colour gradually turned to dark red and powdery mercury also deposited. Stirring was continued until all starting materials were consumed (TLC monitoring, ≈3 h). The reaction mixture was then filtered to remove the very fine powder of mercury and the filtrate was evaporated *in vacuo*. The residue was finally redissolved in CH_2Cl_2 (≈3 cm^3) and separated by preparative TLC using hexane–CH_2Cl_2 (9:1 v/v) as eluent. Four bands were eluted. The first pale yellow band yielded the known cluster $[Os_3(CO)_{10}(\mu\text{-}H)(\mu\text{-}\eta^2\text{-}C{\equiv}CPh)]$ ($R_f \approx 0.7$, 5%), as shown by IR and ^1H NMR spectroscopy. The second red orange band gave *cis*-$[Os(CO)_4\{(\mu\text{-}Hg)Os_3(CO)_{10}(\mu\text{-}\eta^2\text{-}CH{=}CHPh)\}_2]$ **1** ($R_f \approx 0.5$, 30%). Cluster **1** was recrystallised from $CHCl_3$–cyclohexane at room temperature as dark red crystals. The third violet band ($R_f \approx 0.65$) afforded $[\{Os_3(CO)_{10}(\mu\text{-}\eta^2\text{-}CH{=}CHPh)\}_2(\mu_4\text{-}Hg)]$ **2** in 20% yield, crystallised from $CHCl_3$–cyclohexane at room temperature as deep violet crystals. Attempts to characterise the fourth purple band were not successful owing to its instability under ambient conditions. (N.B. repeated TLC using the same eluent was necessary to obtain samples sufficient for accurate spectroscopic as well as structural characterisations.)

Reactions of compound 2

With hydrogen. Hydrogen gas was bubbled through a solution of cluster **2** (40 mg, 0.019 mmol) in refluxing tetrahydrofuran (thf) (5 h) or heptane (3 h). The IR spectrum of the reacting mixture indicated that it contained solely the known cluster $[Os_3(CO)_{10}(\mu\text{-}H)(\mu\text{-}\eta^2\text{-}CH{=}CHPh)]$ accompanied by the deposition of mercury metal.

With $[Hg\{M(CO)_3(\eta^5\text{-}C_5H_5)\}_2]$ (M = Cr, Mo or W). Cluster **2** (50 mg, 0.024 mmol) and $[Hg\{Mo(CO)_3(\eta^5\text{-}C_5H_5)\}_2]$ (17.25 mg, 0.025 mmol) were mixed in freshly distilled hexane (25 cm^3) and refluxed under nitrogen. The reaction was monitored by TLC and after about 30 min a new pale orange band appeared. Reflux was continued for 6–10 h after which the reaction mixture was cooled to room temperature. The solvent was then rotary removed. Extraction using CH_2Cl_2 (3 × 5 cm^3) of the residue gave an orange solution which was then reduced in volume to about 3 cm^3. Purification by TLC (hexane–CH_2Cl_2, 8:2 v/v) afforded $[\{Os_3(CO)_{10}(\mu\text{-}\eta^2\text{-}CH{=}CHPh)\}(\mu_3\text{-}Hg)\{Mo(CO)_3(\eta^5\text{-}C_5H_5)\}]$ **4** ($R_f \approx 0.5$) as the major product (45%). Red rod-like crystals of cluster **4** were obtained from $CHCl_3$–cyclohexane at −20 °C overnight. When $[Hg\{M(CO)_3(\eta^5\text{-}C_5H_5)\}_2]$ (M = Cr or W) was employed under identical reaction conditions, the corresponding analogues of **4** were produced, **3** (M = Cr, 38%) and **5** (M = W, 52%).

^1H NMR monitoring of the conversion of compound 1 into 2

A crystalline sample of cluster **1** (20 mg, 0.0192 mmol) was dissolved in $(CD_3)_2CO$ (3 cm^3) in an NMR tube. Spectra were recorded every 12 h at room temperature for 5 d. Comparison of the resonances with those recorded for authentic samples of **1** and **2** clearly indicated the smooth conversion of **1** into **2** which was complete in 3–5 d.

Reaction of compound 1 with $[Hg\{M(CO)_3(\eta^5\text{-}C_5H_5)\}_2]$ (M = Cr, Mo or W)

Cluster **1** (50 mg, 0.019 mmol) and $[Hg\{Mo(CO)_3(\eta^5\text{-}C_5H_5)\}_2]$ (17.25 mg, 0.025 mmol) were mixed in CH_2Cl_2 (25 cm^3) under nitrogen at room temperature. The orange-red cluster **1** immediately changed to orange while TLC (hexane–CH_2Cl_2, 8:2 v/v) revealed an intense orange band ($R_f \approx 0.5$). The reaction mixture was stirred for 1 h after which TLC using hexane–CH_2Cl_2 (8:2 v/v) gave three bands. The first yellow band yielded the unreacted $[Hg\{Mo(CO)_3(\eta^5\text{-}C_5H_5)\}_2]$ while the second orange band ($R_f \approx 0.5$) yielded cluster **4** (72%). A minor violet band ($R_f \approx 0.7$) was not characterised. Similarly, clusters **3** and **5** were produced in 65 and 76% yield, respectively, when $[Hg\{Cr(CO)_3(\eta^5\text{-}C_5H_5)\}_2]$ and $[Hg\{W(CO)_3(\eta^5\text{-}C_5H_5)\}_2]$ were utilised.

Syntheses of $[RC{\equiv}CHgC{\equiv}CR]$ (R = Ph, Me or Et)

The original method[28] was slightly modified as follows: aryl- or alkyl-mercury(II) chloride (2.0 g) was dissolved in a 95% methanol solution (100 cm^3) of potassium hydroxide and stirred for about 15 min. The remaining insoluble HgRCl was then filtered off. The clear solution of HgRCl was treated with acetylene gas in a round-bottomed flask (250 cm^3) equipped with a gas outlet. The solution immediately became turbid and white precipitate was produced. Acetylene gas was passed in until the solution no longer absorbed it. The resulting white precipitate was then filtered off under suction, washed with water and then 95% methanol. The crude product was recrystallised from methanol to afford white platelets of $[RC{\equiv}CHgC{\equiv}CR]$ (R = Ph, 82; Me, 87; Et, 90%).

Reaction of $[Os_3H_2(CO)_{10}]$ with [PhHgC≡CHgPh]

The compounds [PhHgC≡CHgPh] (33.75 mg, 0.058 mmol) and $[Os_3H_2(CO)_{10}]$ (50 mg, 0.058 mmol) were mixed in thf (25 cm^3) freshly distilled under nitrogen. The purple solution gradually turned to red on stirring and finally to red-brown after 3 h of stirring. The solvent was then removed *in vacuo* and the residue extracted with CH_2Cl_2 (3 × 5 cm^3). The combined extracts were reduced to about 2 cm^3. Isolation by TLC using hexane–CH_2Cl_2 (9:1 v/v) afforded four bands. The first yellow band ($R_f \approx 0.8$) was shown to be $[Os_3(CO)_{12}]$ (5%) by IR spectroscopy and TLC. The second purple band ($R_f \approx 0.72$) yielded $[\{Os_3(CO)_{10}(\mu\text{-}\eta^2\text{-}CH{=}CH_2)\}(\mu_4\text{-}Hg)\{Os_3(CO)_{10}(\mu\text{-}H)\}]$ **6** (12%), which was recrystallised from $CHCl_3$-cyclohexane at room temperature over a period of 1 week as dark purple crystals. The third deep pink band ($R_f \approx 0.55$) was identified as $[\{Os_3(CO)_{10}(\mu\text{-}\eta^2\text{-}CH{=}CH_2)\}_2(\mu_4\text{-}Hg)]$ **7** (25%) and was recrystallised from CH_2Cl_2 by slow evaporation at −20 °C to produce dark red crystals. Attempts to characterise the fourth minor pale red band ($R_f \approx 0.42$) were not successful. Reactions utilizing [RHgC≡CHgR] (R = Me or Et) as reactants also proceed in a similar manner and afforded identical products.

Crystal structure analyses of clusters 1, 2, 4, 6 and 7

Table 13 summarises the relevant data for the crystal structure analyses. The unit-cell parameters were refined by a least-squares procedure. Three standard reflections were monitored periodically throughout data collection and showed no significant variation in each case. All intensity data were corrected for Lorentz, polarisation effects, while absorption corrections by the ψ-scan method were applied for all crystals. The structures were solved by a combination of direct methods (SIR 88)[31] and Fourier-difference techniques and refined on *F* by full-matrix least-squares analysis. The hydrogen atoms of organic moieties were generated in their ideal positions (C–H 0.95 Å), while all metal hydrides were estimated by potential-energy calculations.[32] In cluster **4** a two-fold positional

Table 1 Spectroscopic data for clusters **1–7**

Cluster	IR, $\tilde{\nu}$(CO)[a]/cm^{-1}	^{1}H NMR δ(J/Hz)	Mass, m/z[b]
1	2101w, 2095m, 2072m, 2047vs, 2011s, 1997s, 1980m, 1950w	[c]8.40 (d, J = 14, 2 H, H_v) 7.46 (m, 10 H, H_p) 5.68 (d, J = 14, 2 H, H_v)	2612 (2612)
2	2104m, 2091s, 2050vs, 2008s (br), 1974m	[c]8.33 (d, J = 14, 2 H, H_v) 7.47 (m, 10 H, H_p) 5.85 (d, J = 14, 2 H, H_v)	2108 (2108)
3	2097m, 2047vs, 2013s, 1989m, 1953m, 1896w, 1865m	[c]7.95 (d, J = 14.8, 1 H, H_v) 7.46 (m, 5 H, H_p) 5.80 (d, J = 14.6, 1 H, H_v) 5.63 (s, 5 H, C_5H_5)	1360 (1360)
4	2097m, 2046vs, 2011s, 1989m, 1906w, 1878m	[d]8.15 (d, J = 14.3, 1 H, H_v) 7.39 (m, 5 H, H_p) 5.52 (d, J = 15, 1 H, H_v) 5.41 (s, 5 H, C_5H_5)	1404 (1404)
5	2098m, 2047vs, 2015s, 1988m, 1915w, 1895m	[d]8.36 (d, J = 14.5, 1 H, H_v) 7.22 (m, 5 H, H_p) 5.35 (d, J = 14.7, 1 H, H_v) 5.34 (s, 5 H, C_5H_5)	1491 (1491)
6	2108w, 2093s, 2061vs, 2052s, 2019s, 2004s, 1990s	[d]8.09 (dd, J = 9.06, 1 H, H_v) 4.98 (dd, J = 3.02, 1 H, H_v) 3.55 (dd, J = 3.02, 1 H, H_v) −10.96 (s, 1 H, OsHOs)	1930 (1930)
7	2107m, 2094s, 2051vs, 2013s (br), 1981m (br)	[e]7.95 (dd, J = 9.34, 2 H, H_v) 5.05 (dd, J = 3.02, 2 H, H_v) 3.74 (dd, J = 3.02, 2 H, H_v)	1959 (1959)

[a] Spectra recorded in CH_2Cl_2, v = very, s = strong, m = medium, w = weak, br = broad. [b] Calculated value in parentheses. [c] Recorded in $(CD_3)_2CO$. [d] Recorded in CD_2Cl_2. H_p = phenyl H; H_v = vinyl H. [e] Recorded in $CDCl_3$.

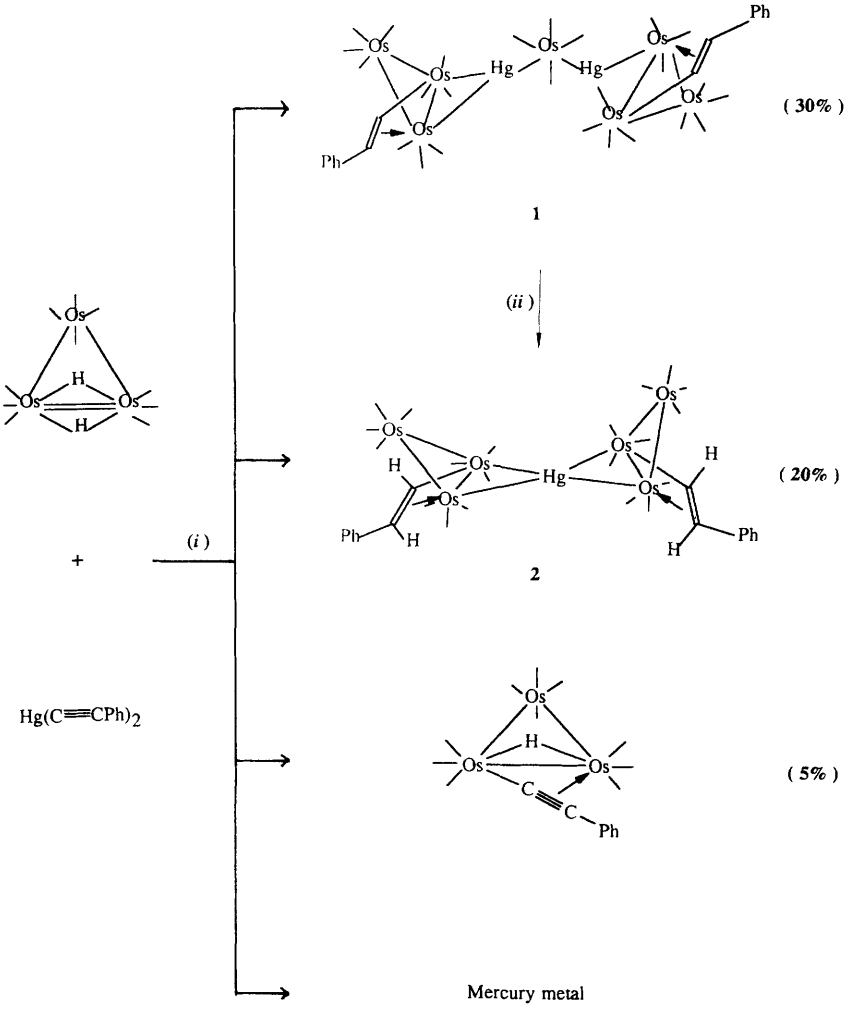

Scheme 3 (*i*) CH_2Cl_2, room temperature, 3 h; (*ii*) acetone, room temperature, 3–5 d

Table 2 Final positional parameters with estimated standard deviations (e.s.d.s) for cluster **1**

Atom	*x*	*y*	*z*	Atom	*x*	*y*	*z*
Hg(1)	0.504 37(7)	0.360 08(7)	0.187 99(3)	C(2)	0.637(2)	0.484(2)	0.253(1)
Os(1)	0.0	0.501 3(1)	0.0	C(3)	0.489(2)	0.453(2)	0.091 8(9)
Os(2)	0.576 86(6)	0.347 74(7)	0.099 91(3)	C(4)	0.678(2)	0.423(2)	0.130 9(9)
Os(3)	0.482 67(6)	0.183 89(7)	0.141 21(3)	C(5)	0.634(2)	0.358(2)	0.043 9(10)
Os(4)	0.684 45(7)	0.171 95(7)	0.112 53(4)	C(6)	0.362(2)	0.191(2)	0.169 9(9)
O(1)	0.497(2)	0.643(2)	0.170(1)	C(7)	0.466(2)	0.059(2)	0.114 5(10)
O(2)	0.722(2)	0.463(2)	0.256 2(9)	C(8)	0.548(2)	0.133(2)	0.191 0(9)
O(3)	0.437(1)	0.518(1)	0.084 1(6)	C(9)	0.725(2)	0.227(2)	0.169(1)
O(4)	0.742(2)	0.471(2)	0.146 7(8)	C(10)	0.800(2)	0.218(2)	0.088(1)
O(5)	0.670(2)	0.362(2)	0.010 0(8)	C(11)	0.726(2)	0.048(2)	0.128(1)
O(6)	0.291(1)	0.189(1)	0.188 6(7)	C(12)	0.633(2)	0.129(2)	0.055(1)
O(7)	0.453(1)	−0.021(1)	0.100 2(7)	C(13)	0.466(2)	0.258(2)	0.072 2(8)
O(8)	0.588(1)	0.104(1)	0.224 0(7)	C(14)	0.368(2)	0.259(2)	0.087 3(8)
O(9)	0.752(1)	0.259(2)	0.204 3(8)	C(15)	0.288(2)	0.204(2)	0.065 9(9)
O(10)	0.869(1)	0.253(1)	0.074 7(7)	C(16)	0.193(2)	0.227(2)	0.078 5(10)
O(11)	0.749(1)	−0.031(2)	0.139 3(7)	C(17)	0.110(2)	0.178(2)	0.05 5(1)
O(12)	0.602(1)	0.098(2)	0.019 6(8)	C(18)	0.123(2)	0.113(2)	0.023 0(10)
O(13)	0.492(2)	−0.128(2)	0.206(1)	C(19)	0.215(2)	0.092(2)	0.011 0(10)
C(1)	0.500(3)	0.582(3)	0.202(2)	C(20)	0.296(2)	0.137(2)	0.030 0(9)

Table 3 Selected bond lengths (Å) and angles (°) for cluster **1**

Hg(1)–Os(1)	2.683(1)	Hg(1)–Os(2)	2.856(1)
Hg(1)–Os(3)	2.803(1)	Os(2)–Os(3)	2.901(1)
Os(2)–Os(4)	2.842(1)	Os(3)–Os(4)	2.927(1)
Os(2)–C(13)	2.09(2)	Os(3)–C(13)	2.29(2)
Os(3)–C(14)	2.41(2)	Os(1)–C(1)	1.81(5)
Os(1)–C(2)	1.88(3)	C(13)–C(14)	1.43(3)
Hg(1)–Os(1)–Hg(1*)	87.09(6)	Os(1)–Hg(1)–Os(2)	134.09(4)
Os(1)–Hg(1)–Os(3)	164.23(5)	Os(2)–Hg(1)–Os(3)	61.63(3)
Os(2)–Os(3)–Os(4)	58.38(3)	Os(2)–Os(4)–Os(3)	60.37(3)
Os(3)–Os(2)–Os(4)	61.25(3)	Hg(1)–Os(2)–Os(3)	58.27(3)
Hg(1)–Os(3)–Os(2)	60.05(3)	Os(1)–C(1)–O(1)	175(4)
Os(1)–C(2)–O(2)	172(2)		

disorder of the CH=CHPh moiety was encountered. Refinement with occupancies of 0.5 for each site converged to $R = 0.031$, $R' = 0.032$. All calculations were performed on a Silicon-Graphics computer with the TEXSAN package.[33] Final atomic coordinates for clusters **1**, **2**, **4**, **6** and **7** are presented in Tables 2, 5, 7, 9 and 10, respectively.

Complete atomic coordinates, thermal parameters and bond lengths and angles have been deposited at the Cambridge Crystallographic Data Centre. See Instructions for Authors, *J. Chem. Soc., Dalton Trans.*, 1996, Issue 1.

Results and Discussion

Synthesis and crystal structures of *cis*-[Os(CO)$_4${(μ-Hg)Os$_3$(CO)$_{10}$(μ-η^2-CH=CHPh)}$_2$] **1** and [{Os$_3$(CO)$_{10}$(μ-η^2-CH=CHPh)}$_2$(μ$_4$-Hg)] **2**

Treatment of the unsaturated cluster [Os$_3$H$_2$(CO)$_{10}$] with 1 equivalent of Hg(C≡CPh)$_2$ in CH$_2$Cl$_2$ at room temperature for 3 h afforded two new Os–Hg clusters **1** and **2** in 30 and 20% yields, respectively (Scheme 3). A small amount of the known cluster [Os$_3$(CO)$_{10}$(μ-H)(μ-η^2-C≡CPh)][34] (5%) and metallic mercury have also been isolated. As shown by ^{1}H NMR spectroscopy (Table 1), both of the C≡C bonds of the ligand moieties have been partially hydrogenated to C=C bonds by rearrangement of the two bridging hydrides of [Os$_3$H$_2$(CO)$_{10}$]. To establish the molecular structures of clusters **1** and **2** we have carried out single-crystal X-ray analyses for them.

The molecular structure of cluster **1** is depicted in Fig. 1. Atomic coordinates are shown in Table 2, selected bond distances and angles in Table 3. The molecule possesses a crystallographic two-fold axis so that half of it is generated by symmetry operation. Cluster **1** comprises a central Os(CO)$_4$ fragment with two *cis*-co-ordinated (μ-Hg)Os$_3$(CO)$_{10}$(μ-η^2-CH=CHPh) units. The geometry around Os(1) is octahedrally distorted, with the C(O)–Os–C(O) angles ranging from 93(1) to 104(2)°. The central Hg(1)–Os(1) and Hg(1*)–Os(1) bond distances [2.683(1) Å] are significantly shorter than the two asymmetric bridging Hg–Os bonds: Hg(1)–Os(2) [2.856(1) Å] and Hg(1)–Os(3) [2.803(1) Å]. Similar shortenings of ruthenium–mercury bonds have been observed in *cis*-[Ru(CO)$_4${(μ-Hg)Ru$_3$(CO)$_9$(μ$_3$-C≡CCMe$_3$)}$_2$] where the difference in the corresponding distances was about 0.16 Å.[14] According to Gadenic,[36] the intramolecular Hg···Hg distance (3.7 Å) and the Hg(1)–Os(1)–Hg(1*) angle [87.09(6)°] both indicate very little interaction between the two *cis*-(μ-Hg)Os$_3$(CO)$_{10}$(μ$_3$-η^2-CH=CHPh) fragments. Such Hg···Hg interaction was observed in *cis*-[Ru(CO)$_4${(μ-Hg)-Ru$_3$(CO)$_9$(μ$_3$-C≡CCMe$_3$)}$_2$][14] (Hg···Hg 3.55 Å and Hg–Ru–Hg 84°) and in *cis*-[Fe(CO)$_4$(HgBr)$_2$][37] (Hg···Hg 3.1 Å and Hg–Fe–Hg 81°). Further examples illustrating the correlation between Hg···Hg distance and Hg–M–Hg angle are shown in Table 4. We can presume that, in general, the shorter the Hg···Hg distances the smaller are the Hg–M–Hg angles and hence the larger the interactions between the two Hg subunits. The geometry around Hg(1) [or Hg(1*)] is trigonal, involving three osmium atoms: Os(1), Os(2) and Os(3). The maximum deviation of 0.004 Å from their least-squares plane indicates that Os(1), Hg(1), Os(2) and Os(3) are almost coplanar. Within each osmium triangle, the variations in the metal–metal bond distances are significant: Os(2)–Os(3) [2.901(1)], Os(2)–Os(4) [2.842(1)] and Os(3)–Os(4) [2.927(1) Å]. In particular, the unsupported Os(3)–Os(4) edge is longer than the mercury-bridged Os(2)–Os(3) bonding edge by 0.026 Å. This may suggest some electron excess on the two atoms Os(3) and Os(4). In fact, electron counting at each osmium atom suggests that Os(3) is the most electron rich. The dihedral angles of the two metal butterflies, as defined by Hg(1), Os(3), Os(2) and Os(4), is 121.07°. The solid-state structure of cluster **1** indicates that the two butterflies and subsequently the two PhCH=CH ligand moieties are arranged in a transoid manner. To our knowledge, the Os–Hg mixed-metal framework of cluster **1** is unprecedented, although an isostructural Ru–Hg carbonyl cluster has been isolated.[14] On the other hand, the ability of Hg to act as a 'linker' in metal-chain structures is again demonstrated. The central Os(CO)$_4$ linkage is most probably derived from partial degradation of the parent Os$_3$(CO)$_{10}$ metal core of the starting material [Os$_3$H$_2$(CO)$_{10}$]. A similar but not strictly comparable example involving the Os(CO)$_4$ linkage was

Table 4 Hg · · · Hg distances and angle Hg–M–Hg in compounds comparable with **1**

Compound	Hg · · · Hg/Å	Hg–M–Hg/°	Ref.
cis-$[Fe(CO)_4(HgBr)_2]$	3.10	81	37
cis-$[Fe(CO)_4(HgSCN)_2]$	3.15	78	38
$[Fe(CO)_4\{HgCl(C_5H_5N)\}_2]$	3.17	77	39
$[Fe(CO)_4(HgSCN)_2(phen)_2]$	3.22	78	40
$[Hg\{Fe(CO)_4(\mu\text{-}Hg)Fe_3(\mu\text{-}COMe)_{10}\}_2]$	3.26	79	13
$[Fe(CO)_4(HgCl_2)(HgCl)]$	3.27	80	41
cis-$[Ru(CO)_4\{(\mu\text{-}Hg)Ru_3(CO)_9(\mu_3\text{-}C{\equiv}CCMe_3)\}_2]$	3.55	84	14
cis-$[Os(CO)_4\{(\mu\text{-}Hg)Os_3(CO)_{10}(\mu\text{-}\eta^2\text{-}CH{=}CHPh)\}_2]$ **1**	3.70	87	This work

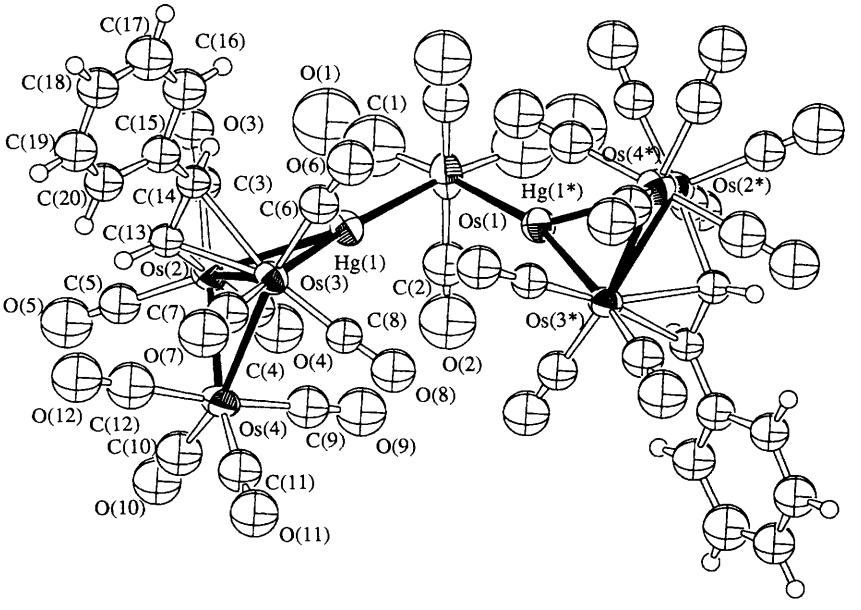

Fig. 1 An ORTEP drawing of *cis*-$[Os(CO)_4\{(\mu\text{-}Hg)Os_3(CO)_{10}(\mu\text{-}\eta^2\text{-}CH{=}CHPh)\}_2]$ **1**

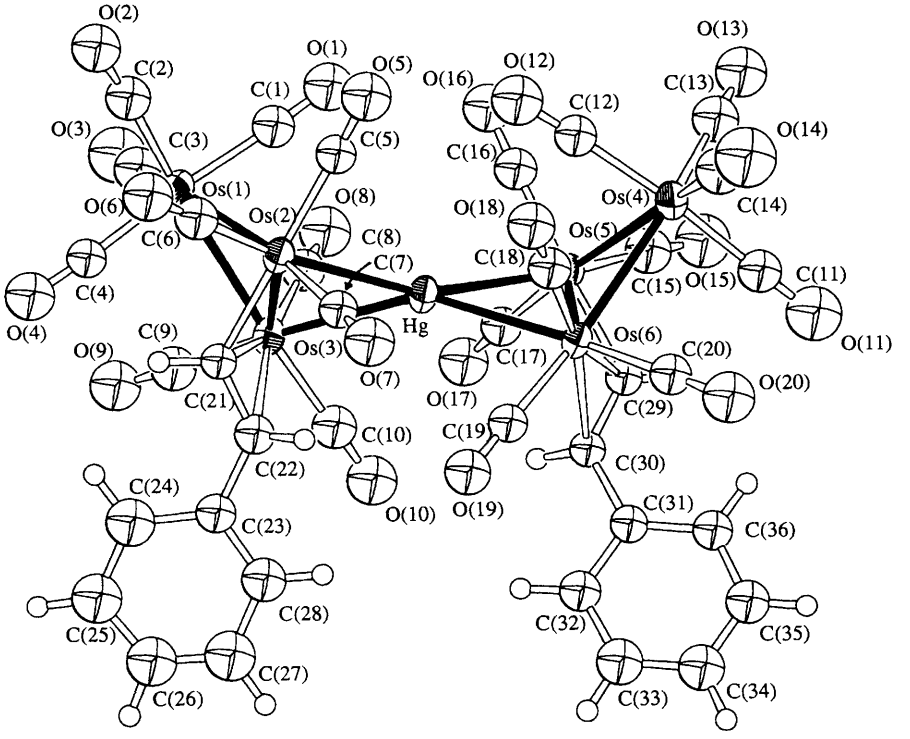

Fig. 2 An ORTEP drawing of $[\{Os_3(CO)_{10}(\mu\text{-}\eta^2\text{-}CH{=}CHPh)\}_2(\mu_4\text{-}Hg)]$ **2**

observed in $[Os_3\{\mu\text{-}AuOs(CO)_4(PPh_3)\}(\mu\text{-}Cl)(CO)_{10}]$ where the gold atom and the PPh_3 ligands are linked in a *trans* configuration through the $Os(CO)_4$ fragment.[42]

The metal framework of cluster **2** consists of two Os–Hg mixed-metal butterflies sharing a central wingtip mercury atom Hg, through which a non-crystallographic two-fold axis passes.

Table 5 Final positional parameters with e.s.d.s for cluster **2**

Atom	*x*	*y*	*z*	Atom	*x*	*y*	*z*
Hg	0.525 51(5)	0.266 77(4)	0.199 22(8)	C(6)	0.789(2)	0.257(1)	−0.023(2)
Os(1)	0.843 39(6)	0.353 38(5)	0.303 01(9)	C(7)	0.602(1)	0.182(1)	−0.055(2)
Os(2)	0.693 54(6)	0.256 15(4)	0.080 13(8)	C(8)	0.694(2)	0.332(1)	0.486(2)
Os(3)	0.713 06(6)	0.235 83(5)	0.376 97(8)	C(9)	0.830(2)	0.218(1)	0.522(2)
Os(4)	0.239 10(6)	0.369 88(5)	0.038 26(9)	C(10)	0.623(2)	0.168(1)	0.440(2)
Os(5)	0.369 82(6)	0.336 82(5)	0.304 54(8)	C(11)	0.124(2)	0.320(1)	0.070(2)
Os(6)	0.324 59(5)	0.215 20(4)	0.056 69(8)	C(12)	0.363(2)	0.413(1)	0.013(2)
O(1)	0.683(1)	0.472 9(9)	0.257(2)	C(13)	0.209(2)	0.473(1)	0.103(2)
O(2)	0.952(1)	0.445 5(9)	0.130(2)	C(14)	0.173(2)	0.364(1)	−0.164(3)
O(3)	0.944(1)	0.442(1)	0.602(2)	C(15)	0.285(2)	0.392(1)	0.396(2)
O(4)	0.998(1)	0.227 3(9)	0.340(2)	C(16)	0.452(2)	0.436(1)	0.324(2)
O(5)	0.609(1)	0.396 4(9)	−0.083(2)	C(17)	0.450(1)	0.308(1)	0.482(2)
O(6)	0.845(1)	0.256 4(9)	−0.089(2)	C(18)	0.358(2)	0.249(1)	−0.108(2)
O(7)	0.552(1)	0.134 9(9)	−0.145(2)	C(19)	0.388(1)	0.118(1)	0.048(2)
O(8)	0.682(1)	0.389 6(9)	0.554(2)	C(20)	0.198(2)	0.173(1)	−0.058(2)
O(9)	0.902(1)	0.209 0(9)	0.608(2)	C(21)	0.752(1)	0.162(1)	0.192(2)
O(10)	0.572(1)	0.130 2(9)	0.484(2)	C(22)	0.699(1)	0.103(1)	0.233(2)
O(11)	0.054(1)	0.292(1)	0.094(2)	C(23)	0.734(1)	0.031(1)	0.302(2)
O(12)	0.437(1)	0.435 4(9)	−0.004(2)	C(24)	0.836(2)	0.018(1)	0.352(2)
O(13)	0.191(1)	0.535 1(10)	0.148(2)	C(25)	0.866(2)	−0.051(1)	0.418(3)
O(14)	0.135(2)	0.357(1)	−0.284(2)	C(26)	0.790(2)	−0.103(1)	0.425(3)
O(15)	0.227(1)	0.422 1(10)	0.447(2)	C(27)	0.696(2)	−0.094(1)	0.382(3)
O(16)	0.497(1)	0.495 6(9)	0.336(2)	C(28)	0.666(2)	−0.024(1)	0.319(2)
O(17)	0.495(1)	0.289 1(9)	0.590(2)	C(29)	0.278(1)	0.230(1)	0.261(2)
O(18)	0.380(1)	0.268 3(8)	−0.204(2)	C(30)	0.307(1)	0.152(1)	0.267(2)
O(19)	0.425(1)	0.059 6(8)	0.039(1)	C(31)	0.241(1)	0.077(1)	0.236(2)
O(20)	0.120(1)	0.144 3(9)	−0.128(2)	C(32)	0.288(2)	0.007(1)	0.264(2)
C(1)	0.741(2)	0.427(1)	0.274(2)	C(33)	0.226(2)	−0.062(1)	0.244(2)
C(2)	0.910(2)	0.414(1)	0.197(2)	C(34)	0.125(2)	−0.063(1)	0.199(2)
C(3)	0.909(2)	0.407(1)	0.491(2)	C(35)	0.081(2)	0.005(1)	0.173(2)
C(4)	0.938(2)	0.272(1)	0.323(2)	C(36)	0.138(1)	0.076(1)	0.193(2)
C(5)	0.639(1)	0.347(1)	−0.015(2)				

Table 6 Selected bond lengths (Å) and angles (°) for cluster **2**

Hg–Os(2)	2.895(1)	Hg–Os(3)	2.823(1)
Hg–Os(5)	2.887(1)	Hg–Os(6)	2.824(1)
Os(2)–Os(3)	2.888(1)	Os(5)–Os(6)	2.89(1)
Os(1)–Os(2)	2.866(1)	Os(1)–Os(3)	2.922(1)
Os(4)–Os(5)	2.860(1)	Os(4)–Os(6)	2.915(1)
Os(2)–C(21)	2.10(2)	Os(3)–C(21)	2.28(2)
Os(3)–C(22)	2.48(2)	Os(5)–C(29)	2.10(2)
Os(6)–C(29)	2.24(2)	Os(6)–C(30)	2.48(2)
C(21)–C(22)	1.38(2)	C(29)–C(30)	1.39(2)
Os(2)–Hg–Os(3)	60.66(3)	Os(5)–Hg–Os(6)	60.81(3)
Hg–Os(2)–Os(3)	58.43(2)	Hg–Os(3)–Os(2)	60.91(3)
Hg–Os(5)–Os(6)	58.51(3)	Hg–Os(6)–Os(5)	60.68(3)
Os(1)–Os(2)–Os(3)	61.04(3)	Os(1)–Os(3)–Os(2)	59.11(3)
Os(2)–Os(1)–Os(3)	59.86(3)	Os(4)–Os(5)–Os(6)	60.90(3)
Os(4)–Os(6)–Os(5)	59.02(3)	Os(5)–Os(4)–Os(6)	60.08(3)

An ORTEP drawing is shown in Fig. 2. Atomic coordinates and some important bond parameters are in Tables 5 and 6, respectively. The two metal butterflies are arranged in the cisoid configuration. However, careful studies showed the butterflies were in fact skewed in such a manner as to minimise the non-bonded interaction between the forward pointing carbonyls on Os(2) and Os(3) with those on Os(5) and Os(6), respectively. In this context, the geometry around the Hg could be described as pseudo-linear[13] and the dihedral angle between the Hg–Os(2)–Os(3) and Hg–Os(4)–Os(5) planes is 52.3°. This value is between those observed in $[\{Os_3(CO)_9(\mu\text{-H})(\mu_3\text{-S})\}_2(\mu_4\text{-Hg})]$[23] (65°) and $[\{Ru_3(CO)_{10}(\mu\text{-NO})\}_2(\mu_4\text{-Hg})]$[43] (27.6°). In the butterflies the dihedral angles between the wings are 125.8 and 124.2° which are slightly larger than the average in $[\{Os_3(CO)_9(\mu\text{-H})(\mu_3\text{-S})\}_2(\mu_4\text{-Hg})]$[23] (114°) and similar to that in $[\{Ru_3(CO)_9(\mu_3\text{-C}{\equiv}CCMe_3)\}_2(\mu_4\text{-Hg})]$[16] (125°). Although the solid-state structure of **2** revealed a cisoid configuration, we cannot disgard the possibility of other structures such as a transoid arrangement present in solution. It has been shown that the energy barrier to such rotation is low.[44] Unfortunately, detailed studies of the fluxional process of cluster **2** by ^{13}C NMR spectroscopy were hampered by its limiting solubilities in the common organic solvents. As in cluster **1**, the unsupported Os(1)–Os(3) [2.922(1)] and Os(4)–Os(6) [2.915(1) Å] edges of the two osmium triangles are substantially elongated. The average Os–Os distance in **2** [2.89(4)] is almost identical to that in **1** [2.89(5)] but is slightly longer than that in $[Os_3(CO)_{12}]$ [2.877(3) Å].[45]

The organic moieties 'CH=CHPh' in clusters **1** and **2** result from Hg–C bond cleavage of the reactant $Hg(C{\equiv}CPh)_2$. Their $\mu\text{-}\eta^2$ bonding mode is reflected in the widespread chemical shift ($\approx\delta$ 2.7) of the two vinyl proton doublets in the ^1H NMR spectra and their *trans* configuration is deduced from the observed coupling constants ($\approx$14 Hz).[34] In cluster **1** the Os(2)–C(13) distance [2.09(2)] and the average of the Os(3)–C(13) and Os(3)–C(14) distances [2.35(2) Å] are indicative of σ and π bonding of the CH=CHPh moiety towards Os(2) and Os(3), respectively. As a whole, the CH=CHPh moieties bridge along the hinged Os–Os edge as three-electron donors to the cluster valence shell. In essence, the structural properties of the triosmium metal domain of clusters **1** and **2** was the same as those found in $[Os_3(CO)_{10}(\mu\text{-H})(\mu\text{-}\eta^2\text{-CH=CHEt})]$,[46] indicating the remarkable rigidity of the metal framework.

Cluster **1** was converted into **2** under ambient conditions smoothly and quantitatively over a period of 3–5 d. The conversion was monitored by ^1H NMR and IR [ν(CO)] techniques (see Experimental section). We are, however, unable to detect any intermediates during the monitoring by ^1H NMR under the experimental conditions. There are two possibilities compatible with this finding. Either the conversion occurs in one step or the intermediate(s) involved are not detectable on the NMR time-scale. Besides, IR studies also indicated no intermediate(s). Thus, we believe that the former possibility is

more likely. At this stage we are unable to offer a detailed mechanism for the conversion.

When hydrogen was bubbled through a solution of cluster **2** in refluxing thf for 5 h, the cluster $[Os_3(CO)_{10}(\mu\text{-}H)(\mu\text{-}\eta^2\text{-}CH{=}CHPh)]$ and mercury were afforded. No reaction was observed at room temperature. Since cluster **2** is thermally stable in refluxing thf, we believe that it reacts directly with hydrogen rather than decomposes thermally before reacting with hydrogen. A similar result has been reported for $[\{Ru_3(CO)_9(\mu_3\text{-ampy})\}_2(\mu_4\text{-Hg})]$ (ampy = 2-aminopyridine).[47]

Synthesis of $[\{Os_3(CO)_{10}(\mu\text{-}\eta^2\text{-}CH{=}CHPh)\}(\mu_3\text{-Hg})\{M(CO)_3(\eta^5\text{-}C_5H_5)\}]$ (M = Cr 3, Mo 4 or W 5)

Asymmetric mercurials **3–5** were synthesised by the reaction of cluster **2** with the symmetric mercurials $[Hg\{M(CO)_3(\eta^5\text{-}C_5H_5)\}_2]$ (M = Cr, Mo or W) (Scheme 4). The reaction proceeded in refluxing thf with an overall yield of 38, 45 and 52%, respectively and no reaction was observed at room temperature. The IR signals associated with the carbonyl ligands at the triosmium framework are virtually identical (Table 1). This indicates that clusters **3–5** are essentially isostructural. On the contrary, signals associated with the carbonyls co-ordinating at M increase stepwise by about 10 cm^{-1} as M goes from Cr, Mo to W. This is certainly related to the decreasing orbital overlap of the occupied nd_π orbitals of M with the π^* antibonding orbitals of the carbonyl ligands. The ^1H NMR spectra (Table 1) all contain signals attributed to vinyl, phenyl as well as C_5H_5 protons but no metal hydride signal. Therefore, oxidative addition to the C–H bond is excluded. In order to establish the molecular structures of the clusters a single-crystal X-ray analysis for **4** was carried out.

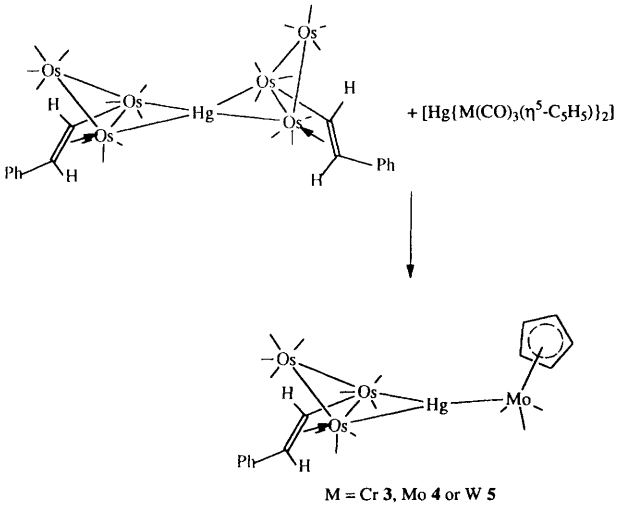

Scheme 4 Formation of clusters **3–5**

Crystal structure of $[\{Os_3(CO)_{10}(\mu\text{-}\eta^2\text{-}CH{=}CHPh)\}(\mu_3\text{-Hg})\{Mo(CO)_3(\eta^5\text{-}C_5H_5)\}]$ 4

An ORTEP drawing of cluster **4** is shown in Fig. 3. Atomic coordinates and related bond parameters are in Tables 7 and 8, respectively. As in clusters **1** and **2**, the metal core comprises a butterfly framework with the Os(2)–Os(3) edge and Os(1) and Hg(1) forming the hinge and the wingtips of the butterfly, respectively. The dihedral angle of the butterfly is 122.46° which is almost identical to that in cluster **1** (121.07°). The Hg(1) atom is triangularly surrounded by two Os atoms and a Mo atom with maximum deviation of 0.11 Å from their least-squares plane. The Hg–Mo distance [2.744(2) Å] is similar to those in $[\{Ru_3(CO)_9(\mu_3\text{-}C{\equiv}CCMe_3)\}(\mu_3\text{-Hg})\{Mo(CO)_3(\eta^5\text{-}C_5H_5)\}]$ [2.743(2) Å] and $[Hg\{Mo(CO)_3(\eta^5\text{-}C_5H_5)\}_2]$ [2.746(2) Å] but significantly longer than that in $[\{Os_3(CO)_9(\mu_3\text{-}C{\equiv}CCMe_3)\}(\mu_3\text{-Hg})\{Mo(CO)_3(\eta^5\text{-}C_5H_5)\}]$ [2.718(3) Å]. The Os(2)–Hg [2.8149(9) Å] and Os(3)–Hg [2.8353(9) Å] bonds are slightly asymmetric as shown by the observed Mo–Hg–Os(2) [147.23(4)°] and Mo–Hg–Os(3) [150.70(4)°] angles. At the Mo, the typical distorted four-legged piano-stool configuration with Hg and the three CO as the legs is retained. The average distance of the apical cyclopentadiene ring from Mo is 2.34 Å. The Mo–Hg bond is offset from the plane defined by Hg, Os(2) and Os(3) by approximately 4.8° in a direction opposite to that of the CH=CHPh moiety (Fig. 4). The CH=CHPh moiety exhibits a two-fold 50% positional disorder and atomic coordinates for the second image of the moiety have also been

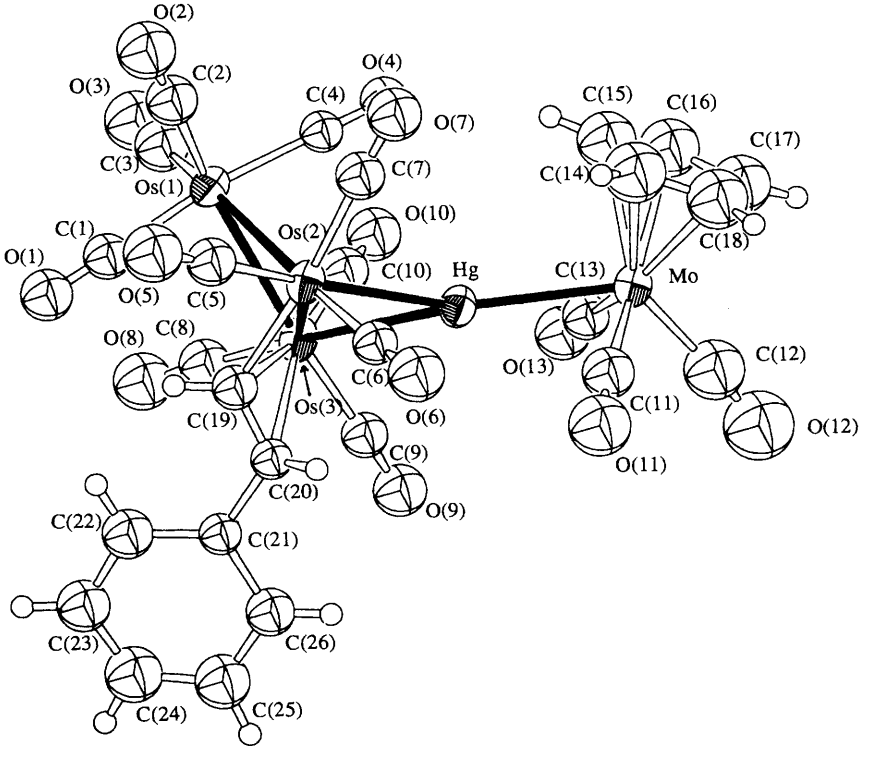

Fig. 3 An ORTEP drawing of $[\{Os_3(CO)_{10}(\mu\text{-}\eta^2\text{-}CH{=}CHPh)\}(\mu_3\text{-Hg})\{Mo(CO)_3(\eta^5\text{-}C_5H_5)\}]$ **4**

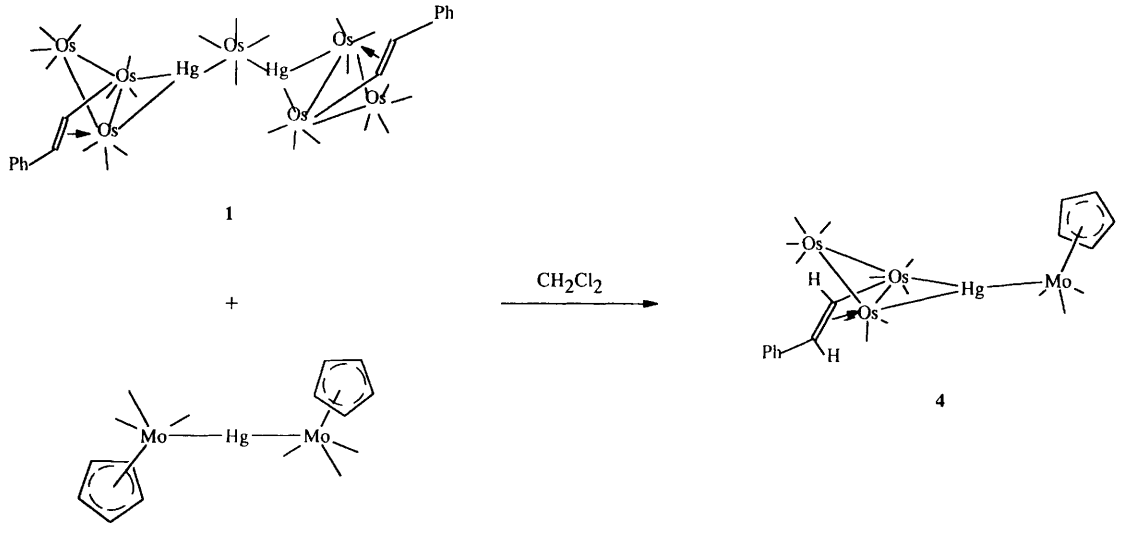

Scheme 5 Alternative pathway for the formation of clusters **3**–**5** from **1**

Table 7 Final positional parameters with e.s.d.s for cluster **4**

Atom	*x*	*y*	*z*	Atom	*x*	*y*	*z*
Hg	0.734 96(5)	0.106 07(4)	0.682 65(7)	C(9)	0.709(1)	0.193(1)	0.365(2)
Os(1)	0.974 37(5)	0.309 39(5)	0.728 38(7)	C(10)	0.919(1)	0.147(1)	0.456(2)
Os(2)	0.762 32(5)	0.285 98(5)	0.822 91(7)	C(11)	0.562(2)	0.002(1)	0.743(2)
Os(3)	0.813 32(5)	0.244 92(5)	0.506 56(7)	C(12)	0.597(2)	−0.149(2)	0.585(3)
Mo	0.691 1(1)	−0.076 9(1)	0.719 4(2)	C(13)	0.747(1)	−0.063(1)	0.515(2)
O(1)	0.910 4(9)	0.511 6(9)	0.631(1)	C(14)	0.747(2)	−0.074(2)	0.982(3)
O(2)	1.067(1)	0.378 9(10)	1.042(2)	C(15)	0.840(2)	−0.084(2)	0.898(2)
O(3)	1.172(1)	0.305(1)	0.551(2)	C(16)	0.842(2)	−0.166(2)	0.816(2)
O(4)	1.015 3(9)	0.098 7(8)	0.797(1)	C(17)	0.750(2)	−0.211(2)	0.848(3)
O(5)	0.780(1)	0.474(1)	1.004(2)	C(18)	0.694(2)	−0.153(2)	0.951(3)
O(6)	0.545(1)	0.248 8(9)	0.932(1)	C(19)	0.721(1)	0.363(1)	0.610(2)
O(7)	0.873 6(10)	0.166 6(9)	1.078(1)	C(20)*	0.637(2)	0.344(2)	0.527(4)
O(8)	0.896(1)	0.373 0(10)	0.286(2)	C(21)*	0.594(2)	0.406(2)	0.401(4)
O(9)	0.655 6(10)	0.162 4(9)	0.268(1)	C(22)*	0.638(3)	0.494(3)	0.373(5)
O(10)	0.977 9(10)	0.087 9(9)	0.420(1)	C(23)*	0.597(4)	0.548(3)	0.251(5)
O(11)	0.479(1)	0.045(1)	0.760(2)	C(24)*	0.517(3)	0.511(3)	0.159(5)
O(12)	0.536(1)	−0.187(1)	0.497(2)	C(25)*	0.468(3)	0.430(3)	0.183(5)
O(13)	0.781 0(10)	−0.059 9(9)	0.395(1)	C(26)*	0.505(3)	0.372(3)	0.301(5)
C(1)	0.931(1)	0.438(1)	0.669(2)	C(27)*	0.621(3)	0.349(2)	0.625(4)
C(2)	1.033(1)	0.351(1)	0.925(2)	C(28)*	0.540(2)	0.431(2)	0.685(3)
C(3)	1.098(2)	0.308(1)	0.618(2)	C(29)*	0.436(3)	0.417(2)	0.690(4)
C(4)	0.999(1)	0.175(1)	0.776(2)	C(30)*	0.368(4)	0.491(3)	0.723(6)
C(5)	0.776(1)	0.402(1)	0.937(2)	C(31)*	0.399(3)	0.580(3)	0.754(4)
C(6)	0.625(1)	0.263(1)	0.884(2)	C(32)*	0.501(4)	0.600(4)	0.748(6)
C(7)	0.834(1)	0.212(1)	0.983(2)	C(33)*	0.578(3)	0.523(2)	0.710(4)
C(8)	0.865(1)	0.321(1)	0.371(2)				

* Occupancy factor 0.5.

Table 8 Selected bond lengths (Å) and angles (°) for cluster **4**

Hg–Os(2)	2.8149(9)	Hg–Os(3)	2.8353(9)
Hg–Mo	2.744(2)	Os(2)–Os(3)	2.8849(8)
Os(1)–Os(2)	2.897(1)	Os(1)–Os(3)	2.8803(9)
Os(2)–C(19)	2.22(2)	Os(3)–C(20)	2.56(2)
Os(3)–C(19)	2.16(2)	Mo–C(12)	1.93(2)
Mo–C(11)	1.93(2)	Mo–C(13)	1.98(2)
C(19)–C(20)	1.28(3)	C(19)–C(27)*	1.30(3)
Hg–Os(2)–Os(3)	59.65(2)	Hg–Os(3)–Os(2)	58.95(2)
Mo–Hg–Os(3)	61.41(2)	Mo–Hg–Os(2)	147.23(4)
Os(1)–Os(3)–Os(2)	60.34(2)	Mo–Hg–Os(3)	150.70(4)
Mo–C(11)–O(11)	174(1)	Os(2)–Os(1)–Os(3)	59.91(2)
Mo–C(13)–O(13)	176(1)	Mo–C(12)–O(12)	174(2)

* Occupancy factor 0.5.

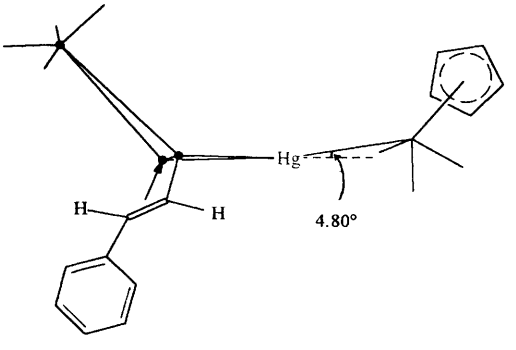

Fig. 4 Offset of the Mo–Hg bond from the Hg–Os(2)–Os(3) plane of cluster **4**

given in Table 7. As mentioned before, clusters **3** and **5** are isostructural with **4**, thus **5** represents a mixed-metal cluster bearing the Os–Hg–W metal linkage. Unfortunately, we were unable to obtain suitable crystals of it for detailed structural analysis.

Although clusters **3**–**5** were successfully prepared *via* the

redistribution pathway, the overall yields are not satisfactory (< 50%) and the reaction rate is rather slow (6–10 h). As suggested by Mays and Robb,[25] this is not unreasonable since the central Hg atom of cluster **2** has already been four-co-ordinated so that redistribution would occur *via* a slower dissociative pathway rather than an alternative faster associative mechanism. Curiously, when cluster **1** was treated with $[Hg\{M(CO)_3(\eta^5\text{-}C_5H_5)\}_2]$ in CH_2Cl_2 under ambient conditions **3–5** were afforded as the major products (Scheme 5). The reaction was essentially complete within 15 mins. This synthetic pathway not only leads to higher yields but also requires less rigorous experimental conditions. Accordingly, we believe that although both reactions give identical products the underlying mechanisms are different.

Synthesis of $[\{Os_3(CO)_{10}(\mu\text{-}\eta^2\text{-}CH{=}CH_2)\}(\mu_4\text{-}Hg)\{Os_3(CO)_{10}(\mu\text{-}H)\}]$ 6 and $[\{Os_3(CO)_{10}(\mu\text{-}\eta^2\text{-}CH{=}CH_2)\}_2(\mu_4\text{-}Hg)]$ 7

To test the generality of the Hg–C bond cleavage observed in the case of $Hg(C{\equiv}CPh)_2$, we have investigated the reaction of $[Os_3H_2(CO)_{10}]$ with another class of organomercury compounds which also possess the nucleophilic –C≡C– functionality, [RHgC≡CHgR] (R = Ph, Me or Et). Treatment of stoichiometric amounts of $[Os_3H_2(CO)_{10}]$ and [RHgC≡CHgR] in CH_2Cl_2 for 3 h afforded $[\{Os_3(CO)_{10}(\mu\text{-}\eta^2\text{-}CH{=}CH_2)\}(\mu_4\text{-}Hg)\{Os_3(CO)_{10}(\mu\text{-}H)\}]$ **6** and $[\{Os_3(CO)_{10}(\mu\text{-}\eta^2\text{-}CH{=}CH_2)\}_2(\mu_4\text{-}Hg)]$ **7** in 12 and 25% yields respectively (Scheme 6). Infrared spectroscopy [ν(CO)] indicates that the metal framework of cluster **7** is quite similar to that of **2**. However, signals corresponding to the protons of the R groups are not observed in their respective ^1H NMR spectra. Instead, three sets of double doublets indicative of three vinyl protons appeared. For cluster **6** an intense hydride singlet at δ −10.96 is also observed. We believe that the anticipated Hg–C bond cleavage has occurred. In order to establish the molecular structures of clusters **6** and **7** X-ray analyses were carried out.

Molecular structures of compounds 6 and 7

The ORTEP drawings of clusters **6** and **7** are depicted in Figs. 5 and 6, respectively. Atomic coordinates are listed in Tables 9 and 10, selected bond distances and angles in Tables 11 and 12, respectively. In cluster **7**, as a consequence of Hg–C bond cleavage, only the $CH{=}CH_2$ moiety (from partial hydrogenation of the C≡C moiety of [PhHgC≡CHgPh]) is co-ordinated to the osmium triangle. In fact, clusters **2** and **7** are isostructural with regard to their metal framework, see Figs. 2 and 6. In this context, the average dihedral angles of the two butterflies, the twist angle about the central Hg atom and the average Os–Os bond distance in cluster **7** are 126.2, 52.9° and 2.89(3) Å, respectively, which are almost identical to those in cluster **2** [125.0, 52.3° and 2.89(4) Å]. Consequently, it is reasonable to presume that both clusters adopt a skewed cisoid configuration in their solid-state structures. The average π-co-ordinating $CH{=}CH_2$ distance [1.39(4) Å] and the average σ-co-ordinating Os–C bond distance [2.06(1) Å] are not unusual as compared with the corresponding values in $[Os_3(CO)_{10}(\mu\text{-}H)(\mu\text{-}\eta^2\text{-}CH{=}CH_2)]$ [1.396(4) and 2.107(3) Å, respectively].[48] In cluster **6** the two osmium triangles defined by Os(4), Os(5), Os(6) and Os(1), Os(2), Os(3) are strikingly different. The former is structurally identical to the two triangles in cluster **7** while the latter bears solely a bridging hydride at the hinged Os(2)–Os(3) edge. In contrast to those in clusters **2** and **7**, the two butterflies are mutually transoid, as in the case of $[\{Ru_3(CO)_9(\mu_3\text{-}C{\equiv}CCMe_3)\}_2(\mu_4\text{-}Hg)]$.[16] The Os(2)–Os(3) distance [2.708(1) Å] is rather short. In fact, the effective atomic number rule[49] suggests that this edge should comprise a metal–metal double bond and hence there should be a total of four metal–metal bonds within the Os(1)–Os(2)–Os(3) triangle, as in $[Os_3H_2(CO)_{10}]$ where the Os=Os distance is 2.680(1) Å.[50] An example in which a hydride and an HgR moiety bridge across two adjacent Os–Os edges in an Hg–Os cluster is found in $[\{Os_3(CO)_9(\mu\text{-}H)(\mu_3\text{-}S)\}_2(\mu_4\text{-}Hg)]$.[23]

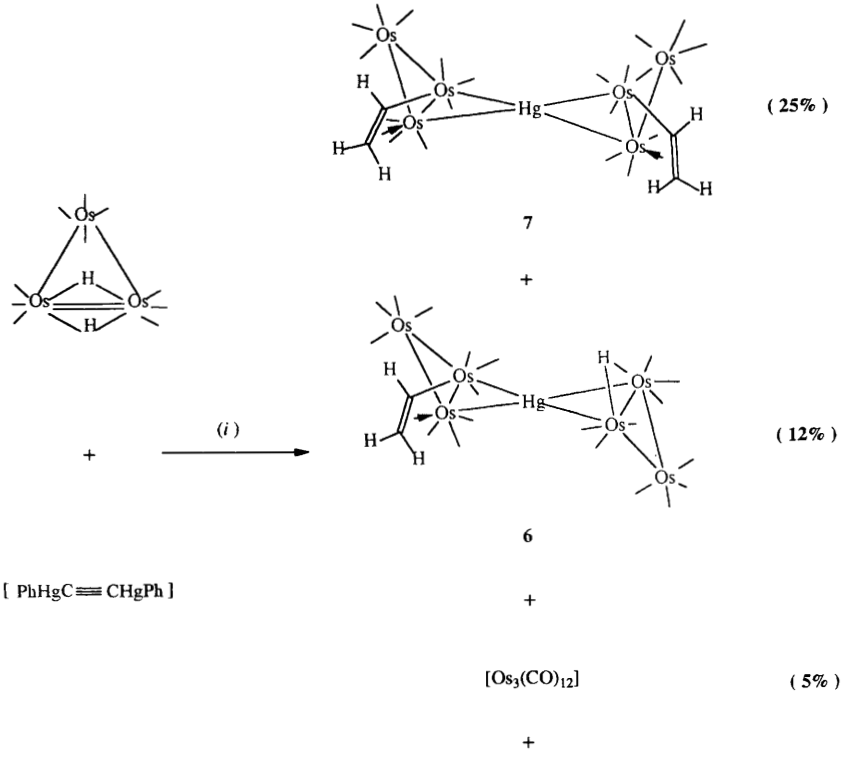

Scheme 6 (i) CH_2Cl_2, room temperature, 3 h

Table 9 Final positional parameters with e.s.d.s for cluster **6**

Atom	*x*	*y*	*z*	Atom	*x*	*y*	*z*
Hg	0.479 38(8)	0.259 47(5)	0.776 21(9)	O(19)	0.668(2)	0.353(1)	0.490(2)
Os(1)	0.219 47(10)	0.425 72(6)	0.598 0(1)	O(20)	0.602(2)	0.102(1)	0.468(2)
Os(2)	0.250 62(9)	0.335 81(5)	0.844 32(9)	C(1)	0.179(2)	0.531(1)	0.689(3)
Os(3)	0.276 64(9)	0.255 20(6)	0.571 80(9)	C(2)	0.210(3)	0.445(2)	0.389(3)
Os(4)	0.784 6(1)	0.080 81(6)	0.862 1(1)	C(3)	0.058(2)	0.395(1)	0.588(3)
Os(5)	0.654 26(9)	0.218 88(6)	1.002 56(10)	C(4)	0.387(2)	0.441(1)	0.630(2)
Os(6)	0.717 47(9)	0.223 13(6)	0.704 43(10)	C(5)	0.327(2)	0.424(1)	0.949(3)
O(1)	0.152(2)	0.596(1)	0.745(2)	C(6)	0.108(2)	0.381(1)	0.909(3)
O(2)	0.205(2)	0.457(1)	0.269(3)	C(7)	0.269(2)	0.264(1)	0.992(2)
O(3)	−0.037(2)	0.376(1)	0.588(2)	C(8)	0.297(2)	0.145(2)	0.579(3)
O(4)	0.488(2)	0.450(1)	0.651(2)	C(9)	0.154(3)	0.245(2)	0.421(3)
O(5)	0.371(2)	0.480(1)	1.010(2)	C(10)	0.386(3)	0.259(2)	0.430(3)
O(6)	0.021(2)	0.412(1)	0.957(2)	C(11)	0.790(3)	0.011(2)	1.021(3)
O(7)	0.276(2)	0.224(1)	1.087(2)	C(12)	0.863(3)	0.008(2)	0.727(3)
O(8)	0.309(2)	0.074(1)	0.585(2)	C(13)	0.928(3)	0.129(2)	0.946(3)
O(9)	0.082(2)	0.239(1)	0.323(2)	C(14)	0.633(3)	0.045(2)	0.782(3)
O(10)	0.457(2)	0.256(1)	0.348(2)	C(15)	0.586(2)	0.314(1)	1.097(3)
O(11)	0.790(2)	−0.024(1)	1.117(3)	C(16)	0.749(3)	0.197(2)	1.176(3)
O(12)	0.920(2)	−0.036(1)	0.645(3)	C(17)	0.538(3)	0.143(2)	1.035(3)
O(13)	1.015(2)	0.157(1)	0.994(2)	C(18)	0.870(2)	0.195(2)	0.649(3)
O(14)	0.541(2)	0.024(1)	0.739(2)	C(19)	0.682(2)	0.307(1)	0.577(2)
O(15)	0.544(2)	0.375(1)	1.159(2)	C(20)	0.652(2)	0.145(1)	0.561(3)
O(16)	0.803(2)	0.187(1)	1.283(2)	C(21)	0.786(2)	0.286(1)	0.930(3)
O(17)	0.470(2)	0.101(1)	1.056(2)	C(22)	0.750(3)	0.350(2)	0.849(3)
O(18)	0.964(2)	0.179(1)	0.604(2)				

Table 10 Final positional parameters with e.s.d.s for cluster **7**

Atom	*x*	*y*	*z*	Atom	*x*	*y*	*z*
Hg	0.297 3(1)	0.100 98(10)	0.262 02(7)	O(20)	0.250(2)	0.155(2)	0.022(1)
Os(1)	0.463 9(1)	0.227 7(1)	0.410 76(7)	C(1)	0.485(4)	0.473(3)	0.228(2)
Os(2)	0.412 9(1)	0.330 3(1)	0.252 48(8)	C(2)	0.697(4)	0.486(3)	0.377(2)
Os(3)	0.700 6(1)	0.345 4(1)	0.319 60(8)	C(3)	0.813(5)	0.405(4)	0.225(3)
Os(4)	0.057 1(1)	−0.077 0(1)	0.267 08(8)	C(4)	0.510(4)	0.276(3)	0.150(2)
Os(5)	0.223 8(1)	−0.058 4(1)	0.108 72(7)	C(5)	0.694(4)	0.201(3)	0.266(2)
Os(6)	0.164 8(2)	−0.263 0(1)	0.187 79(9)	C(6)	0.847(4)	0.334(3)	0.397(2)
O(1)	0.516(4)	0.571(3)	0.218(2)	C(7)	0.233(5)	0.312(4)	0.197(3)
O(2)	0.700(3)	0.571(2)	0.411(2)	C(8)	0.574(5)	0.301(3)	0.513(3)
O(3)	0.875(3)	0.447(3)	0.164(2)	C(9)	0.297(3)	0.169(3)	0.472(2)
O(4)	0.546(3)	0.243(2)	0.089(2)	C(10)	0.534(3)	0.093(3)	0.410(2)
O(5)	0.691(2)	0.111(2)	0.237(1)	C(11)	−0.003(4)	0.039(3)	0.333(2)
O(6)	0.941(3)	0.337(2)	0.448(2)	C(12)	0.154(3)	−0.114(3)	0.366(2)
O(7)	0.129(3)	0.306(3)	0.158(2)	C(13)	−0.104(5)	−0.184(4)	0.274(3)
O(8)	0.633(3)	0.339(2)	0.579(2)	C(14)	0.104(4)	−0.361(3)	0.273(2)
O(9)	0.199(3)	0.128(2)	0.511(2)	C(15)	−0.004(5)	−0.319(4)	0.114(3)
O(10)	0.578(3)	0.015(2)	0.413(2)	C(16)	0.240(4)	−0.359(3)	0.113(3)
O(11)	−0.049(4)	0.104(3)	0.378(2)	C(17)	0.349(4)	−0.197(3)	0.247(2)
O(12)	0.213(3)	−0.134(2)	0.429(2)	C(18)	0.187(3)	−0.148(3)	0.004(2)
O(13)	−0.216(4)	−0.245(3)	0.294(2)	C(19)	0.425(3)	−0.049(2)	0.106(2)
O(14)	0.069(3)	−0.422(3)	0.329(2)	C(20)	0.241(4)	0.075(3)	0.055(2)
O(15)	−0.110(4)	−0.345(3)	0.074(2)	C(21)	0.264(4)	0.373(3)	0.367(2)
O(16)	0.305(4)	−0.405(3)	0.062(2)	C(22)	0.394(3)	0.368(3)	0.397(2)
O(17)	0.461(3)	−0.163(3)	0.279(2)	C(23)	−0.058(4)	0.005(3)	0.161(2)
O(18)	0.164(3)	−0.201(2)	−0.065(2)	C(24)	0.008(3)	−0.076(3)	0.121(2)
O(19)	0.538(3)	−0.049(2)	0.097(2)				

Table 11 Selected bond lengths (Å) and angles (°) for cluster **6**

Hg–Os(2)	2.883(2)	Hg–Os(3)	2.838(2)
Os(2)–Os(3)	2.708(1)	Os(1)–Os(2)	2.829(1)
Os(1)–Os(3)	2.836(1)	Hg–Os(5)	2.845(1)
Hg–Os(6)	2.840(2)	Os(5)–Os(6)	2.888(1)
Os(4)–Os(5)	2.857(1)	Os(4)–Os(6)	2.928(1)
Os(6)–C(21)	2.30(2)	Os(6)–C(22)	2.38(3)
Os(5)–C(21)	2.14(2)		
Hg–Os(2)–Os(3)	60.89(3)	Hg–Os(3)–Os(2)	62.60(4)
Os(2)–Hg–Os(3)	56.51(4)	Os(1)–Os(2)–Os(3)	61.58(3)
Os(1)–Os(3)–Os(2)	61.31(3)	Os(2)–Os(1)–Os(3)	57.11(3)
Hg–Os(5)–Os(6)	59.39(4)	Hg–Os(6)–Os(5)	59.56(3)
Os(5)–Hg–Os(6)	61.05(4)	Os(4)–Os(5)–Os(6)	61.30(3)
Os(4)–Os(6)–Os(5)	58.83(3)	Os(5)–Os(4)–Os(6)	59.87(3)

Table 12 Selected bond lengths (Å) and angles (°) for cluster **7**

Hg–Os(1)	2.890(2)	Hg–Os(2)	2.836(2)
Os(1)–Os(2)	2.904(2)	Os(1)–Os(3)	2.860(2)
Os(2)–Os(3)	2.925(2)	Hg–Os(4)	2.829(2)
Hg–Os(5)	2.899(2)	Os(4)–Os(5)	2.905(2)
Os(4)–Os(6)	2.936(2)	Os(5)–Os(6)	2.851(2)
Os(1)–C(22)	2.05(3)	Os(2)–C(21)	2.37(3)
Os(2)–C(22)	2.22(3)	Os(5)–C(24)	2.07(3)
Os(4)–C(23)	2.38(3)	Os(4)–C(24)	2.27(3)
C(21)–C(22)	1.36(5)	C(23)–C(24)	1.42(4)
Hg–Os(1)–Os(2)	58.60(4)	Hg–Os(2)–Os(1)	60.44(4)
Os(1)–Hg–Os(2)	60.95(4)	Os(1)–Os(2)–Os(3)	58.77(4)
Os(2)–Os(1)–Os(3)	60.97(4)	Os(1)–Os(3)–Os(2)	60.26(4)
Hg–Os(5)–Os(4)	58.33(4)	Hg–Os(4)–Os(5)	60.73(4)
Os(4)–Hg–Os(5)	60.93(4)	Os(5)–Os(4)–Os(6)	58.43(4)
Os(4)–Os(5)–Os(6)	61.34(5)	Os(4)–Os(6)–Os(5)	60.24(4)

Table 13 Crystal data for clusters **1**, **2**, **4**, **6** and **7***

	1	**2**	**4**	**6**	**7**
Empirical formula	$C_{40}H_{14}HgO_{20}Os_7 \cdot 2H_2O$	$C_{36}H_{14}HgO_{20}Os_6$	$C_{26}H_{12}HgMoO_{13}Os_3$	$C_{22}H_4HgO_{20}Os_6$	$C_{24}H_6HgO_{20}Os_6$
Colour, habit	Red orange, prism	Reddish violet, block	Red, long rod	Black, prism	Red, block
Crystal size/mm	0.24 × 0.42 × 0.44	0.28 × 0.33 × 0.41	0.10 × 0.12 × 0.42	0.22 × 0.25 × 0.33	0.32 × 0.34 × 0.38
Crystal system	Monoclinic	Triclinic	Triclinic	Triclinic	Triclinic
Space group	$C2/c$ (no. 15)	$P\bar{1}$ (no. 2)	$P\bar{1}$ (no. 2)	$P\bar{1}$ (no. 2)	$P\bar{1}$ (no. 2)
a/Å	13.612(1)	13.988(2)	12.631(3)	11.363(5)	9.717(2)
b/Å	13.766(1)	16.864(7)	14.254(4)	16.583(4)	12.479(3)
c/Å	29.734(3)	9.735(1)	8.698(2)	9.139(6)	15.167(3)
α/°	90.0	96.56(2)	93.08(2)	96.94(4)	94.80(2)
β/°	93.25(2)	105.93(1)	93.57(2)	94.97(5)	90.52(2)
γ/°	90.0	92.21(2)	85.87(2)	85.43(3)	103.48(2)
U/Å^3	5562.9(7)	2188(1)	1557.1(6)	1698(1)	1781.4(6)
Z	4	2	2	2	2
M	2647.14	2108.28	1399.50	1930.05	1956.09
D_c/g cm^{-3}	3.162	3.201	2.985	3.773	3.646
μ/cm^{-1}	215.19	209.48	175.67	269.23	256.78
F(000)	4632	1852	1244	1664	1692
Diffractometer	Enraf-Nonius CAD4	Rigaku AFC7R	Rigaku AFC7R	Rigaku AFC7R	Enraf-Nonius CAD4
2θ Range/°	2–45	4–45	4–45	4–45	2–45
Scan speed/° min^{-1} (in ω)	1.06–16.48	16.0	16.0	16.0	1.37–16.48
Scan range (ω)	0.70 + 0.35 tan θ	1.21 + 0.35 tan θ	1.15 + 0.35 tan θ	1.42 + 0.35 tan θ	0.80 + 0.35 tan θ
Reflections collected	4018	5993	4304	4611	4980
Independent reflections	3874	5710	4078	4343	4648
Observed reflections [$I > 3\sigma(I)$]	2493	4262	2944	3098	3269
Weighting scheme factor, p	0.002	0.002	0.002	0.005	0.012
R,R' (observed data)	0.041, 0.051	0.034, 0.039	0.031, 0.032	0.036, 0.036	0.055, 0.066
Goodness of fit, S	2.010	1.871	1.600	2.062	2.451
Largest Δ/σ	0.01	0.01	0.04	0.01	0.01
Number of parameters	174	288	230	232	240
Residual extrema in the final difference map/e Å^{-3}	2.00 to −1.06 close to Hg and Os	1.02 to −1.53 close to Os	1.24 to −0.93 close to Os	1.90 to −1.41 close to Os	2.88 to −3.61 close to Os and Hg

* Details in common: Mo-Kα radiation (λ = 0.710 73 Å); T 295 K; ω–2θ scans; background measurement 25% at both ends; $w = 4F_o^2/[\sigma^2(F_o^2) + p(F_o^2)^2]$.

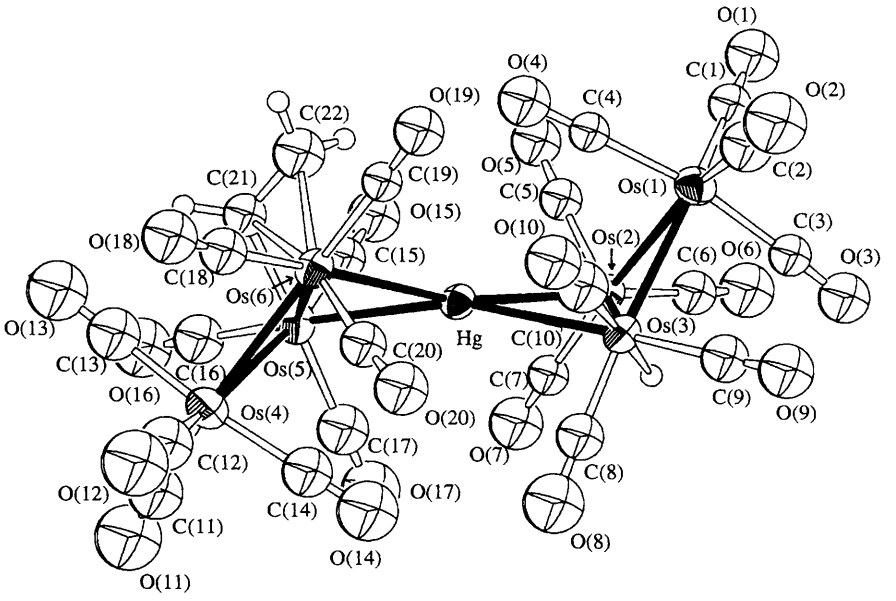

Fig. 5 An ORTEP drawing of $[\{Os_3(CO)_{10}(\mu\text{-}\eta^2\text{-}CH{=}CH_2)\}(\mu_4\text{-}Hg)\{Os_3(CO)_{10}(\mu\text{-}H)\}]$ **6**

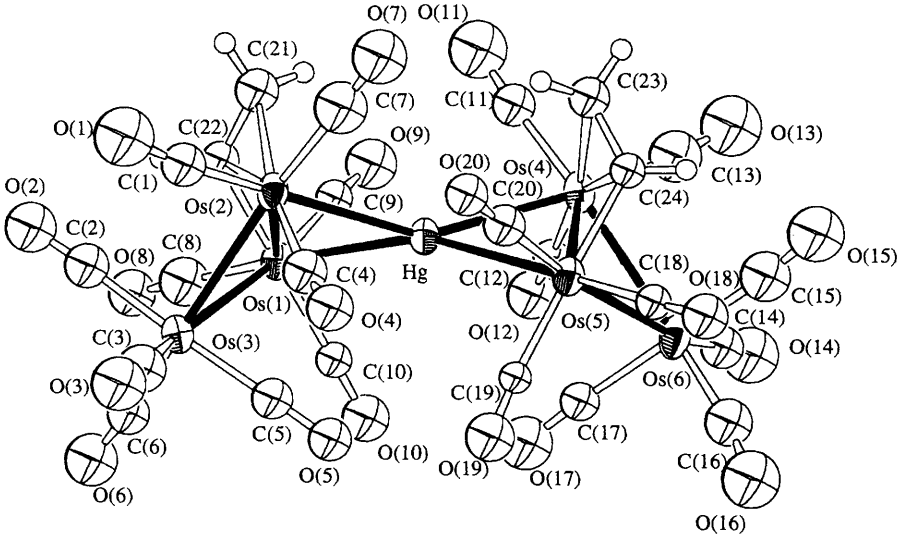

Fig. 6 An ORTEP drawing of $[\{Os_3(CO)_{10}(\mu\text{-}\eta^2\text{-}CH{=}CH_2)\}_2(\mu_4\text{-}Hg)]$ **7**

Acknowledgements

W.-T. W. acknowledges financial support from the Research Grants Council and the University of Hong Kong and Y.-K. A. acknowledges the receipt of a postgraduate studentship, administered by The University of Hong Kong.

References

1 M. Fajardo, H. D. Holden, B. F. G. Johnson, J. Lewis and P. R. Raithby, *J. Chem. Soc., Chem. Commun.*, 1984, 24.
2 J. M. Ragosta and J. M. Burlitch, *J. Chem. Soc., Chem. Commun.*, 1985, 1187; *Organometallics*, 1986, **5**, 1517; 1988, **7**, 1469.
3 S. R. Drake, K. Henrick, B. F. G. Johnson, J. Lewis, M. McPartlin and J. Morris, *J. Chem. Soc., Chem. Commun.*, 1986, 928.
4 L. H. Gade, B. F. G. Johnson, J. Lewis, M. McPartlin and H. R. Powell, *J. Chem. Soc., Chem. Commun.*, 1990, 110; *J. Chem. Soc., Dalton Trans.*, 1992, 921.
5 J. Strahle and K. Wurst, *Z. Anorg. Allg. Chem.*, 1991, **595**, 239.
6 B. F. G. Johnson, W. L. Kwik, J. Lewis, P. R. Raithby and V. P. Saharan, *J. Chem. Soc., Dalton Trans.*, 1991, 1037.
7 T. Tanase, T. Horiuchi, Y. Yamamoto and K. Kobayashi, *J. Organomet. Chem.*, 1992, **440**, 1.
8 L. H. Gade, *Angew. Chem., Int. Ed. Engl.*, 1993, **32**, 24.
9 Y. Yamamato and H. Yamazaki, *Inorg. Chim. Acta*, 1994, **217**, 121.
10 Z. Zheng, C. B. Knobler, C. E. Curtis and M. F. Hawthorne, *Inorg. Chem.*, 1995, **34**, 432; F. Teixidor, J. A. Ayllon, C. Vinas, R. Kivekas, R. Sillanpaa and J. Casabo, *J. Organomet. Chem.*, 1994, **483**, 153.
11 M. Ferrer, A. Perales, O. Rossel and M. Seco, *J. Chem. Soc., Chem. Commun.*, 1990, 1447.
12 L. N. Zakharov, Y. T. Struchkov, S. N. Titova, V. T. Bychkov, G. A. Domrachev and G. A. Razumaez, *Cryst. Struct. Commun.*, 1980, **9**, 549.
13 A. Bianchini and L. J. Farrugia, *Organometallics*, 1992, **11**, 540.
14 E. Rosenberg, D. Ryckman, I.-Nan Hsu and R. W. Gellert, *Inorg. Chem.*, 1986, **25**, 194.
15 R. Fahmy, K. King, E. Rosenberg, A. Tiripicchio and M. Tiripicchio-Camellini, *J. Am. Chem., Soc.*, 1980, **102**, 3626.
16 S. Ermer, K. King, K. I. Hardcastle, E. Rosenberg, A. M. M. Lanfredi, A. Tiripicchio and M. T. Camellini, *Inorg. Chem.*, 1983, **22**, 1339.
17 P. Braunstein, J. Rose, A. Tiripicchio and M. Tiripicchio-Camellini, *J. Chem. Soc., Chem. Commun.*, 1984, 391.

18 Y. Yamamoto, H. Yamazaki and T. Sakurai, *J. Am. Chem. Soc.*, 1982, **104**, 2329.
19 E. Charalambous, L. H. Gade, B. F. G. Johnson, T. Kotch, A. J. Lees, J. Lewis and M. McPartlin, *Angew. Chem., Int. Ed. Engl.*, 1990, **10**, 1137.
20 L. H. Gade, B. F. G. Johnson, J. Lewis, M. McPartlin, T. Kotch and A. J. Lees, *J. Am. Chem. Soc.*, 1991, **113**, 8698.
21 E. Rosenberg, J. Wang and R. W. Gellert, *Organometallics*, 1988, **7**, 1093.
22 Y. K. Au and W. T. Wong, *J. Chem. Soc., Dalton Trans.*, 1995, 1389.
23 E. Rosenberg, K. I. Hardcastle, M. W. Day, R. Gobetts, S. Hajela and R. Muftikian, *Organometallics*, 1991, **10**, 203.
24 O. Rossell, M. Seco, G. Segales, S. Alvarez, M. A. Pellinghelli and A. Tiripicchio, *Organometallics*, 1994, **13**, 2205.
25 M. J. Mays and J. D. Robb, *J. Chem. Soc. A*, 1968, 329.
26 J. A. Iggo and M. J. Mays, *J. Chem. Soc., Dalton Trans.*, 1984, 643.
27 G. Eglington, *J. Chem. Soc.*, 1963, 2295.
28 R. J. Spahr, R. R. Vogt and J. A. Nieuwland, *J. Am. Chem. Soc.*, 1933, **55**, 2465.
29 J. M. Burlitch and A. Ferrari, *Inorg. Chem.*, 1970, **9**, 563.
30 W. T. Wong, Ph. D. Thesis, University of Cambridge, 1991.
31 M. C. Burla, M. Camalli, G. Cascarano, C. Giacovazzo, G. Polidori, R. Spagna and P. Viterbo, *J. Appl. Crystallogr.*, 1989, **22**, 389.
32 A. G. Orpen, *J. Chem. Soc., Dalton Trans.*, 1980, 2509.
33 TEXSAN, Crystal Structure Analysis Package, Molecular Structure Corporation, Houston, TX, 1985 and 1992.
34 A. J. Deeming, S. Hasso and M. Underhill, *J. Chem. Soc., Dalton Trans.*, 1975, 1614.
35 C. K. Johnson, ORTEP, Report ORNL-5138, Oak Ridge National Laboratory, Oak Ridge, TN, 1976.
36 B. Grdenic, *Q. Rev. Chem. Soc.*, 1965, **19**, 303.
37 H. W. Baird and L. F. Dahl, *J. Organomet. Chem.*, 1967, **7**, 503.
38 A. E. Mauro, R. H. A. Santos, M. T. P. Gambardella and R. H. P. Francisco, *Polyhedron*, 1987, **6**, 1273.
39 R. W. Baker and P. Pauling, *Chem. Commun.*, 1970, 573.
40 A. E. Mauro, S. H. Pulcinelli, R. H. A. Santos and M. T. P. Gambardella, *Polyhedron*, 1992, **11**, 799.
41 P. D. Brotherton, D. L. Kepert, A. H. White and S. B. Wild, *J. Chem. Soc., Dalton Trans.*, 1976, 1870.
42 C. Cathey, J. Lewis, P. R. Raithby and M. C. Ramirez de Arellano, *J. Chem. Soc., Dalton Trans.*, 1994, 3331.
43 M. P. Gomez-Sal, B. F. G. Johnson, J. Lewis, P. R. Raithby, S. N. Azman and B. Syed-Mustaffa, *J. Organomet. Chem.*, 1984, **272**, C21.
44 S. Hajela, B. M. Novak and E. Rosenberg, *Organometallics*, 1989, **8**, 468.
45 M. R. Churchill and B. G. Deboer, *Inorg. Chem.*, 1977, **16**, 878.
46 J. J. Guy, B. E. Reichert and G. M. Sheldrick, *Acta Crystallogr., Sect. B*, 1976, **32**, 3319.
47 P. L. Andreu, J. A. Cabeza, A. Llamazares, V. Riera, C. Bois and Y. Jeannin, *J. Organomet. Chem.*, 1991, **420**, 431.
48 A. G. Orpen, D. Dippard, G. M. Sheldrick and K. D. Rouse, *Acta Crystallogr., Sect. B*, 1978, **34**, 2466.
49 D. M. P. Mingos and D. J. Wales, *Introduction to Cluster Chemistry*, Prentice-Hall, Englewood Cliffs, NJ, 1990, ch. 2, p.72.
50 A. G. Orpen, A. V. Rivera, E. G. Bryan, D. Pippard, G. M. Sheldrick and K. D. Rouse, *J. Chem. Soc., Chem. Commun.*, 1978, 723; R. W. Broach and J. M. Williams, *Inorg. Chem.*, 1979, **18**, 314.

Received 6*th July* 1995; *Paper* 5/04395F